NIH Public Access
Author Manuscript
J Mol Neurosci. Author manuscript; available in PMC 2010 January 1.

Published in final edited form as:
J Mol Neurosci. 2009 January ; 37(1): 6–15. doi:10.1007/s12031-008-9088-0.

Novel N-terminal Cleavage of APP Precludes Aβ Generation in ACAT-Defective AC29 Cells

Henri J. Huttunen,
Neurobiology of Disease Laboratory, Genetics, and Aging Research Unit, MassGeneral Institute for Neurodegenerative Disease (MIND) and Department of Neurology, Massachusetts General Hospital, Harvard Medical School, Charlestown, MA 02129, USA

Luigi Puglielli,
Neurobiology of Disease Laboratory, Genetics, and Aging Research Unit, MassGeneral Institute for Neurodegenerative Disease (MIND) and Department of Neurology, Massachusetts General Hospital, Harvard Medical School, Charlestown, MA 02129, USA

Blake C. Ellis,
Neurobiology of Disease Laboratory, Genetics, and Aging Research Unit, MassGeneral Institute for Neurodegenerative Disease (MIND) and Department of Neurology, Massachusetts General Hospital, Harvard Medical School, Charlestown, MA 02129, USA

Laura A. MacKenzie Ingano, and
Neurobiology of Disease Laboratory, Genetics, and Aging Research Unit, MassGeneral Institute for Neurodegenerative Disease (MIND) and Department of Neurology, Massachusetts General Hospital, Harvard Medical School, Charlestown, MA 02129, USA

Dora M. Kovacs
Neurobiology of Disease Laboratory, Genetics, and Aging Research Unit, MassGeneral Institute for Neurodegenerative Disease (MIND) and Department of Neurology, Massachusetts General Hospital, Harvard Medical School, Charlestown, MA 02129, USA, e-mail: Dora_Kovacs@hms.harvard.edu

Abstract

A common pathogenic event that occurs in all forms of Alzheimer's disease is the progressive accumulation of amyloid β-peptide (Aβ) in brain regions responsible for higher cognitive functions. Inhibition of acyl-coenzyme A: cholesterol acyltransferase (ACAT), which generates intracellular cholesteryl esters from free cholesterol and fatty acids, reduces the biogenesis of the Aβ from the amyloid precursor protein (APP). Here we have used AC29 cells, defective in ACAT activity, to show that ACAT activity steers APP either toward or away from a novel proteolytic pathway that replaces both α and the amyloidogenic β cleavages of APP. This alternative pathway involves a novel cleavage of APP holoprotein at Glu281, which correlates with reduced ACAT activity and Aβ generation in AC29 cells. This sterol-dependent cleavage of APP occurs in the endosomal compartment after internalization of cell surface APP. The resulting novel C-terminal fragment APP-C470 is destined to proteasomal degradation limiting the availability of APP for the Aβ generating system. The proportion of APP molecules that are directed to the novel cleavage pathway is regulated by the ratio of free cholesterol and cholesteryl esters in cells. These results suggest that subcellular

© Humana Press 2008

Correspondence to: Dora M. Kovacs.

Present address: L. A. MacKenzie Ingano, Merck Research Laboratories, Boston, MA 02115, USA
Present address: L. Puglielli, Department of Medicine, University of Wisconsin-Madison, and Geriatric Research Education Clinical Center, VA Medical Center, Madison, WI 53705, USA

NIH-PA Author Manuscript
NIH-PA Author Manuscript
NIH-PA Author Manuscript

NIH-PA Author Manuscript

NIH-PA Author Manuscript

NIH-PA Author Manuscript

cholesterol distribution may be an important regulator of the cellular fate of APP holoprotein and that there may exist several competing proteolytic systems responsible for APP processing within the endosomal compartment.

Keywords

Alzheimer's disease; Amyloid; Cholesterol

Introduction

Alzheimer's disease (AD) is a neurodegenerative disorder characterized by abnormal deposition of insoluble protein aggregates in brain regions responsible for memory and cognitive functions. Senile plaques constitute the majority of extracellular deposits and are mainly composed of the amyloid β-peptide (Aβ; Glenner and Wong 1984). Aβ is a 39–43 amino acid hydrophobic polypeptide, proteolytically derived from a larger precursor, the amyloid precursor protein (APP; Kang et al. 1987Tanzi et al. 1987). For Aβ biogenesis, APP is first cleaved at the N-terminus of Aβ peptide by β-site APP-cleaving enzyme 1 (BACE1; β cleavage), producing a 99-amino-acid C-terminal fragment (C99). APP can also be cleaved in the middle of the Aβ sequence (nonamyloidogenic α cleavage by cell surface metallo proteases ADAM 10 and ADAM 17) generating an 83-amino-acid C-terminal fragment of APP (C83). Both C99 and C83 are substrates for a subsequent γ cleavage by presenilin-dependent γ-secretase that releases the APP intracellular domain (AICD) and either Aβ peptide (from C99) or p3 peptide (from C83; Haass 2004).

Over the last 15 years, cholesterol metabolism has been established as a major risk factor for AD by genetic (Corder et al. 1993; Schmechel et al. 1993; Ehnholm et al. 1986; Boerwinkle et al. 1987), epidemiological (Jarvik et al. 1995; Kuo et al. 1998; Notkola et al. 1998; Koudinov et al. 1998; Jick et al. 2000; Wolozin et al. 2000), and biochemical (Refolo et al. 1991; Lee et al. 1998; Parkin et al. 1999) studies. In addition, both animal (Refolo et al. 2000, 2001; Fassbender et al. 2001; Hutter-Paier et al. 2004) and cellular (Simons et al. 1998; Frears et al. 1999; Fassbender et al. 2001; Puglielli et al. 2001) models of AD have shown that cholesterol homeostasis and distribution regulate APP processing and Aβ generation (for a review, see Puglielli et al. 2003). Interestingly, recent reports suggest that both APP-derived end products of γ-secretase, Aβ and AICD, may regulate cholesterol homeostasis. $A\beta_{40}$ was shown to inhibit 3-hydroxy-3-methylglutaryl-coenzyme A reductase (Grimm et al. 2005), a rate-limiting enzyme in cholesterol biosynthesis, whereas AICD was shown to regulate brain apolipoprotein E and cholesterol metabolism through transcriptional repression of low-density lipoprotein receptor-related protein 1 (Liu et al. 2007). Thus, the relationship between APP and lipid homeostasis appears to be bidirectional and complicated.

We have previously provided genetic, biochemical, and metabolic evidence that intracellular cholesterol distribution regulates Aβ generation (Puglielli et al. 2001). Acylcoenzyme A: cholesterol acyltransferase (ACAT), the enzyme that generates cholesteryl esters (CEs) from fatty acids and free cholesterol (FC), modulates Aβ production by maintaining a delicate balance between FC and CEs (Hutter-Paier et al. 2004; Huttunen et al. 2007a; Puglielli et al. 2001). Importantly, ACAT inhibitors strongly reduce amyloid pathology correlating with improved cognitive performance in transgenic mouse models of AD (Hutter-Paier et al. 2004; Huttunen et al. 2008, manuscript submitted). Thus, understanding the molecular events linking ACAT inhibition to reduced Aβ generation is important for both a better understanding of the pathogenesis of AD and the development of novel therapeutic strategies for its treatment.

NIH-PA Author Manuscript

NIH-PA Author Manuscript

NIH-PA Author Manuscript

Cholesterol mutant Chinese hamster ovary (CHO) cell lines have been widely used to dissect cellular pathways regulating cholesterol homeostasis (Chang et al. 2006). We have previously used two CHO-based cholesterol mutant cell lines 25RA and AC29 to obtain genetic evidence that ACAT activity regulates APP processing and Aβ generation (Puglielli et al. 2001). Both 25RA and AC29 constitutively generate the active form of sterol-regulatory-element binding protein (SREBP), thus unable to turn off the biosynthesis and uptake of cholesterol (reviewed in Brown and Goldstein 1999; Chang et al. 2006). Consequently, 25RA and AC29 cells overproduce and accumulate cholesterol in a sterol-independent fashion, reaching a two to fourfold increase in total cholesterol content. 25RA cells have increased CE (~6-fold) but normal FC content (Puglielli et al. 2001). AC29 cells were generated from 25RA cells (Cadigan et al. 1988) by an additional loss-of-function mutation in *SOAT1* (the gene encoding ACAT1) which renders AC29 cells incapable of CE generation, resulting in a ~4-fold increase in FC and undetectable CE. Consistent with changes in CE levels, we found that Aβ generation and both α- and β-secretase cleavages are increased in 25RA cells but almost completely blocked in AC29 cells as compared to wild-type CHO cells (Puglielli et al. 2001). Moreover, ACAT inhibitor treatment of three different cell lines as well as primary cortical neurons reduced CEs by approximately 50%, with a corresponding 40–50% reduction in the rate of α and β cleavages and Aβ secretion.

In the current study, we have used ACAT-defective AC29 cells to characterize a novel, sterol-sensitive proteolytic cleavage pathway for APP. We found that in ACAT-defective cells cleavage of APP at Glu281 is required to direct APP to a nonamyloidogenic pathway reducing the availability of APP to α and β cleavages and Aβ generation.

Methods

Cell culture and antibodies

Wild-type and cholesterol mutant (AC29 and 25RA) CHO cell lines were grown in Dulbecco's Modified Eagle Medium and Nutrient Mixture F-12 Ham (Sigma Chemicals Co., St. Louis, MO, USA), respectively. Media were supplemented with 10% (*v/v*) fetal bovine serum (Atlanta Biologicals, Norcross, GA, USA), 1% (*v/v*) L-glutamine–penicillin–streptomycin solution (Sigma), and 0.4% (*v/v*) G418 Sulfate (Calbiochem, La Jolla, CA, USA) as selection marker for cells stably transfected with cDNA constructs expressing APP_{751} or APP (ES/AA) and hygromycin for APP_{C470}-V5/His in a pSec Tag/FRT/V5/His TOPO expression vector (Invitrogen). Cells were cultured at 37°C in a water-saturated air/5% CO_2 atmosphere.

The following antibodies against APP were used throughout this study: 22C11 (monoclonal, against N-terminus; Chemicon); 369 (monoclonal, against C-terminus; generous gift from Dr. Sam Gandy, Mount Sinai School of Medicine, New York, NY, USA); C7 and C8 (against C-terminus; generous gift from Dr. Dennis Selkoe, Harvard Medical School, Boston, MA, USA); 4G8 (monoclonal, against residues 18–25 of Aβ; Endogen); 6E10 (monoclonal, against residues 1–17 of Aβ; Senetek). Antibodies against calreticulin (ER marker), GM130 (Golgi marker), and EEA-1 (early endosomes) were obtained from StressGen Biotechnologies and BD Transduction Laboratories. Anti-V5 antibody was from Invitrogen. β-secretase inhibitor Z-VLL-CHO and ALLN were from Calbiochem and lactacystin, ammonium chloride, chloroquine, methyl-β-cyclodextrin, and mevastatin from Sigma.

Cholesterol determinations

For the determinations of intracellular pools of FC and CE, cells were first incubated ad equilibrium (for 3 days) in the presence of [^{14}C]acetic acid (57.0 mCi/mmol; Amersham Life Science), then washed twice in phosphate-buffered saline (PBS) and extracted in chloroform–methanol (2:1; *v/v*). The chloroform phase was dried, resuspended again in chloroform, and

NIH-PA Author Manuscript

NIH-PA Author Manuscript

NIH-PA Author Manuscript

applied with standards to a Silica Gel-G (EM Science) thin layer chromatography. Plates were developed in hexane–ethyl ether–acetic acid (87:20:1, *v/v*) and visualized with I_2 vapor. Spots were scraped and counted in a liquid scintillation counter.

Subcellular fractionation

Subcellular fractionation was performed as described previously (Puglielli et al. 2001; Huttunen et al. 2007b). Briefly, AC29 cells were washed in PBS, harvested in ice-cold 10 mM 4-(2-hydroxyethyl)-1-piperazineethanesulfonic acid, pH 7.4, 0.25 M sucrose, 1 mM ethylene diamine tetraacetic acid (EDTA) and homogenized using a metal Dounce homogenizer. Postnuclear supernatants (1,500×*g*) cells were fractionated on a 8–34% continuous iodixanol gradients (OptiPrep; Axis-Shield) by centrifugation at 27,000 rpm in a SW41 rotor for ~18 h at 4°C. The 0.8 ml fractions were collected and resolved in 4–12% Bis-Tris sodium dodecyl sulfate-polyacrylamide electrophoretic gels (Novex–Invitrogen).

Biotinylation of cell surface proteins

To label cell surface proteins, growing cells were incubated with EZ-Link™ Sulfo-NHS-LC-Biotin (Pierce) for 45 min at 15°C. Cells were then washed twice in PBS, scraped, and extracted on ice in Triton-Nonidet P-40 buffer containing 10 mM Tris–HC1, pH 6.8, 1 mM EDTA, 150 mM NaCl, 0.25% Nonidet P-40, 1% Triton X-100, and a protease inhibitor cocktail (Roche Applied Science). Biotinylated proteins were separated from nonbiotinylated proteins using BioMag Streptavidin beads (Qiagen), electrophoresed on 4–12% Bis-Tris gel and probed with C7 antibody.

Aβ determinations

For Aβ determination, CHO, 25RA, or AC29 cells stably transfected with APP 14constructs were grown on six-well plates (BD Biosciences). At ~80–90% confluency, cells were washed in PBS and incubated in 1 ml of fresh, complete medium for 24 h. Secreted $A\beta_{total}$ and $A\beta_{42}$ were quantitated by standard sandwich enzyme linked immunosorbent assay (ELISA; Aβ ELISA Core Facility, Center for Neurological Diseases, Harvard Institutes of Medicine, Harvard Medical School).

Statistical analysis

Statistical analyses were performed using Student's *t* test with significance placed at $p<0.05$.

Results

Two Novel, Sterol-Sensitive N-terminal Cleavages of APP in AC29 Cells

Inhibition of ACAT activity by either pharmacological or genetic means reduces generation of Aβ and the APP-CTFs C99 and C83 in various cell types (Puglielli et al. 2001; Huttunen et al. 2007a). As shown in Fig. 1a, both C99 and C83 were almost completely absent in AC29 cells expressing human APP. Treatment of AC29 cells with γ-secretase inhibitor DAPT revealed an accumulation of both C99 and C83 (data not shown). Together with our previously published work (Puglielli et al. 2001), these results indicate that α-, β-, and γ-secretase activities are intact in these cells (see also later on in Fig. 4d). We reasoned that the lack of ACAT activity in AC29 cells may regulate availability of APP holoprotein to α- and β-secretases, possibly by directing APP toward alternative pathways of proteolytic processing. Using an antibody directed against the last 20 amino of human APP (C7; Puglielli et al. 2001; Podlisny et al. 1991), we noticed two novel APP-CTFs in AC29 cells, undetectable in either wild-type CHO or 25RA cells (Fig. 1a, *arrowheads*). These two new fragments, appearing as bands with molecular masses of ~55 and ~85 kDa, were also visible with 6E10 (against amino acids 1–17 of the Aβ region), 4G8 (against amino acids 18–25 of the Aβ region), and 369 (against the C-

NIH-PA Author Manuscript

NIH-PA Author Manuscript

NIH-PA Author Manuscript

terminus of APP) antibodies but not with 22C11 antibody (against the N-terminus of APP; amino acids 66–81; data not shown).

In order to assess whether the generation of the 55- and 85-kDa APP-CTFs in AC29 cells was regulated by ACAT activity, we treated 25RA cells with the competitive ACAT inhibitor CP-113,818. ACAT inhibition progressively shifted cholesterol from the pool of CE to that of FC in this cholesterol-overproducing cell line (Fig. 1b). After 3 weeks of CP-113,818 treatment, FC-to-CE ratio in 25RA cells had reached the level observed in AC29 cells (Fig. 1b; in AC29 cells FC 1,014.8±128.1 and CE 27.1 ± 1.2 mg/g protein, in 25RA cells treated for 3 weeks FC 1,221.7± 157.6 and CE: 130.5 ± 17.2 mg/g, in untreated 25RA cells FC 253.7±32.0 and CE 1,268.5±93.6 mg/g). As expected, absence of ACAT activity almost completely abolished Aβ secretion into the media [Fig. 1c; $A\beta_{total}$ decreased from 14,647.1±1,911.8 to 2,823.5±882.4 pg/ml per milligram protein ($p<0.05$) and $A\beta_{42}$ from 3,029.6±672.4 to 184.7±7.4 pg/ml per milligram protein ($p<0.05$) after the 3-week treatment]. Reduced Aβ secretion paralleled with a decrease in the steady-state levels of C99 and C83 (Fig. 1d). In addition, the 55- and 85-kDa APP-CTFs were visible after 3 weeks of ACAT inhibition, while totally absent in untreated 25RA cells (Fig. 1d). These results indicate that the generation of both the 55- and 85-kDa APP-CTFs is dynamically regulated by ACAT activity and that their production correlates with inhibition of the normal amyloi-dogenic processing of APP. The 55-kDa form of APP appeared as the most prominent ACAT-regulated APP-CTF in these and subsequent experiments.

ACAT inhibition reduces CEs with a concomitant increase in FC levels in 25RA cells (Fig. 1 B). To establish whether the generation of the 55- and 85-kDa APP-CTFs was affected by FC in the absence of changes in CEs, we depleted AC29 cells of cholesterol using a combination of methyl β-cyclodextrin (mβ-CD), a sterol-binding molecule, and mevastatin, an HMG-CoA reductase inhibitor. In our studies, mβ-CD was used for 24 h to allow for cellular cholesterol to reach equilibrium. Cell viability was not affected, as assessed by the release of the cytosolic enzyme lactate-dehydrogenase into the media (data not shown). Mevastatin alone did not induce significant changes in cholesterol levels (data not shown), whereas mβ-CD alone reduced but did not normalize FC levels (Fig. 2a; $p<0.05$ vs untreated control). Only the combination of mβ-CD and mevastatin was able to normalize FC levels (Fig. 2a; $p<0.05$ vs untreated control; also compare to wild-type CHO cells). Normalization of FC levels was followed by a marked increase in both the secretion of Aβ into the media (Fig. 2b; mβ-CD + mevastatin vs untreated control $p<0.05$) and the steady-state levels of C99 and C83 in cells (Fig. 2c), indicating that FC levels are responsible, at least in part, for the reduced generation of Aβ observed in AC29 cells. However, normalized FC in AC29 cells only recovered ~50% of the Aβ secretion as compared to wild-type CHO cells (Fig. 2b). The missing ~50% was presumably due to the absence of CE synthesis in these cells. Importantly, both 55- and 85-kDa APP-CTFs were undetectable after successful normalization of FC (Fig. 2c). To summarize, in three different cellular models (untreated AC29 cells, ACAT inhibitor-treated 25RA cells, and mβ-CD–mevastatin-treated AC29 cells), we consistently observed a membrane cholesterol-sensitive appearance of the 55- and 85-kDa APP-CTFs that inversely correlated with the levels of C99, C83, and Aβ.

Sterol-Sensitive Cleavage of APP Occurs After its Internalization From the Cell Surface in AC29 Cells

AC29 cells have no obvious defect in APP expression, maturation, or transport along the secretory–endocytic compartments (Puglielli et al. 2001). However, it is possible that a small percentage of APP is mislocalized in AC29 cells. In order to determine the cellular compartment where the novel 55- and 85-kDa APP-CTFs are generated, intracellular membranes obtained from AC29 cells stably transfected with APP were subjected to

NIH-PA Author Manuscript

NIH-PA Author Manuscript

NIH-PA Author Manuscript

subcellular fractionation in a continuous OptiPrep gradient. Fractions corresponding to endosomes and Golgi (fractions 1–6 in Fig. 3a) were combined, and fractions containing ER membranes (fractions 7–14 in Fig. 3a) were pooled together to analyze APP localization. The 55-kDa fragment of APP was only detected in the fractions corresponding to the endosomal compartment and Golgi apparatus, whereas the 85-kDa APP-CTF was detected in those corresponding to the ER (Fig. 3b). A Nicodenz continuous gradient, which separates membranes from the Golgi and the endosomal compartments more efficiently, revealed that the 55-kDa form of APP comigrates with markers of both the endosomal and late (trans) Golgi compartments but mainly associates with endosomes (data not shown).

To evaluate whether the generation of the 55-kDa APP-CTF requires cell surface exposure and reinternalization into endosomes, we performed cell surface biotinylation experiments. Biotinylation of cell surface proteins at 15°C did not reveal biotinylated 55-kDa APP-CTF (Fig. 3c). As ε-amino groups available for biotinylation are present throughout the APP ectodomain (including the 55-kDa APP-CTF), this result indicates that the proteolytic cleavage responsible for 55-kDa APP-CTF generation does not occur on the cell surface. Both exocytosis and endocytosis are blocked at 15°C but are immediately reactivated once cells are returned to permissive temperature (37°C). Biotinylated 55-kDa APP-CTF could be detected once cells were replaced at 37°C after biotinylation at 15°C (Fig. 3c), further supporting that generation of the 55-kDa fragment of APP occurs following internalization of cell surface APP in AC29 cells. These data also show that the subpopulation of APP that undergoes the novel, sterol-sensitive cleavage pathway instead of α- and β-secretase cleavages is exposed to the extracellular milieu on the cell surface and correctly undergoes endocytosis. Small changes in endosomal com-partmentalization, causing BACE1 (β-secretase) to lose access to APP, could possibly account for our results.

To assess whether the 55-kDa APP-CTF undergoes proteasomal or lysosomal degradation, AC29 cells stably transfected with APP were first treated with the proteasome inhibitor ALLN, in the presence or absence of β-secretase inhibitor. ALLN alone increased the steady-state levels of C99 but not C83 (Fig. 3d). This effect was completely reversed when Z-VLL-CHO, a selective inhibitor of BACE1 activity (Abbenante et al. 2000), was used in addition to ALLN. The combined use of ALLN and Z-VLL-CHO produced a marked increase in the levels of 55-kDa APP-CTF, which was not evident when Z-VLL-CHO was used alone (Fig. 3d). These data suggest that when the proteosome is inhibited by ALLN, the 55-kDa APP-CTF is stabilized but can still be processed by BACE1. These data also show that BACE1 activity itself is not compromised in AC29 cells. Very similar results were obtained when lactacystin, a more selective inhibitor of proteasomes, was used instead of ALLN. In contrast, no effect was observed when lysosomal inhibitors, chloroquine and ammonium chloride, were used (Fig. 3e). The 85-kDa APP-CTFs (in Fig. 3d, e) were visible only after long exposures (data not shown). Taken together, these results indicate that the 55-kDa APP-CTF is generated after internalization of cell surface APP, most likely in the endosomal compartment, and is then degraded by the proteasome machinery. Whether the 55-kDa APP-CTF is targeted to the proteasome directly from the endosomal compartment or after retrotransport to the ER remains to be determined.

Cleavage at Glu281 of APP Mediates ACAT-Sensitive Reduction of Aβ Generation in AC29 Cells

Since the 55-kDa fragment of APP consistently appeared as the most prominent band of the two novel APP-CTFs, we further characterized the role of this fragment in the ACAT-mediated regulation of Aβ generation. N-terminal sequencing and amino acid composition analysis revealed that the 55-kDa APP-CTF begins at Ser282 of APP yielding a CTF harboring 470 amino acids from the 751 amino acid splice form of APP (Fig. 4a). In analogy to other well-

NIH-PA Author Manuscript

NIH-PA Author Manuscript

NIH-PA Author Manuscript

characterized APP-CTFs, the new 55-kDa APP-CTF generated by cleavage at Glu281 was named "C470". Attempts to sequence the 85-kDa APP-CTF were unsuccessful because of very low recovery of this protein, likely due to its molecular instability.

To establish whether the cleavage of APP at Glu281 could modulate Aβ generation, we stably transfected AC29 cells with a cDNA construct harboring two point mutations in the Glu281 cleavage site of APP. The point mutations E281A and S282A (ES/AA) abolished the generation of APP-C470 while reactivating both β and α cleavages of APP in AC29 cells (Fig. 4b). More importantly, the cells recovered their ability to produce and secrete Aβ [Fig. 4c; $A\beta_{total}$ increased from 913.0±434.5 pg/ml per milligram protein in AC29–APP_{wt} cells to 9,185.0 ±1,018.6 pg/ml per milligram protein in AC29–$APP_{ES/AA}$ cells ($p<0.001$)]. Interestingly, stable transfection of wild-type CHO cells with APP (ES/AA) also produced a modest (~25%) increase in Aβ secretion as compared to CHO–APP_{wt} cells [Fig. 4c; $A\beta_{total}$ secretion in CHO–$APP_{ES/AA}$ cells was 11,390.0±1,780.0 pg/ml per milligram protein as compared to 9,025.3 ±924.7 pg/ml per milligram protein in CHO–APP_{wt} cells ($p>0.05$)]. These data suggest that the protease responsible for generation of APP-C470 may be active in normocholesterolemic, wild-type CHO cells, despite the fact that APP-C470 is undetectable in these cells.

To further characterize the functional significance of the Glu281 cleavage of APP, we stably transfected both wild-type CHO and AC29 cells with a deletion mutant form of APP, missing the amino acids 1–281. The resulting cDNA construct expressed APP-C470 with a V5-His tag at its C-terminal tail (Fig. 4a). As expected, processing of APP*C470*-V5/His was normal in wild-type CHO cells in terms of Aβ, C99, and C83 generation (Fig. 4d, e). Surprisingly, however, AC29 cells stably transfected with APP*C470*-V5/His completely recovered their ability to generate Aβ and cleave APP at both α and β sites (Fig. 4d, e). $A\beta_{total}$ secretion in AC29–APP_{C470} cells was 8,046.0±901.0 pg/ml per milligram protein as compared to 51.2 ±22.2 pg/ml per milligram protein in AC29–APP_{wt} cells ($p<0.01$) and 8,458.3±1,021.7 pg/ml per milligram protein in CHO–APP_{wt} cells ($p<0.01$). $A\beta_{42}$ secretion in AC29–APP_{C470} cells was 990.7±103.5 pg/ml per milligram protein as compared to 31.2±1.3 pg/ml per milligram protein in AC29–APP_{wt} cells ($p<0.01$), and 938.0±100.5 pg/ml per milligram protein in CHO–APP_{wt} cells ($p<0.01$). These data indicate that APP-C470 can act as a substrate for both α- and β-secretases, independent of ACAT activity. Taken together with the previous data, these results suggest that ACAT-sensitive reduction of Aβ generation requires both the N-terminal 1–281 amino acids and Glu281 cleavage of APP in AC29 cells.

Discussion

Cholesterol is known to modulate the activity and processing of a wide array of membrane proteins. It regulates the proteolytic processing of SREBPs (reviewed in Brown and Goldstein 1999) and HMG-CoA reductase (Fitzky et al. 2001), modulates the interaction of INSIG-1 with SCAP (Yang et al. 2002) and HMG-CoA-reductase (Sever et al. 2003), is covalently linked to the Hedgehog protein (Porter et al. 1996), and binds to synaptophysin (Thiele et al. 2000) and caveolin (Murata et al. 1995). Understanding how APP fits into this long list of proteins regulated by cholesterol may shed new light on the pathophysiology of AD. Reduction of ACAT activity suppresses Aβ generation in cell and animal models of AD. Here, by using AC29 cells as a model system, we identify a novel sterol-dependent cleavage pathway for APP. The lack of ACAT activity in AC29 cells results in two novel proteolytic cleavages in the N-terminal domain of APP, the most predominant of which occurs after Glu281. This novel cleavage pathway almost completely abolishes Aβ generation by diverting APP away from the α-, β-, and γ-secretases. The cleavage of APP at Glu281 occurs after internalization of cell surface APP and may involve rapid proteasomal degradation of the resulting APP-C470 fragment.

NIH-PA Author Manuscript

NIH-PA Author Manuscript

NIH-PA Author Manuscript

Changes in secreted Aβ correlate with changes in CE but not always with FC, although FC is in equilibrium with CE, complicating clear distinctions at the molecular level. Independent of the specific molecular events involving CE versus FC, our previous work has established a major role for ACAT activity in the modulation of APP processing via at least α- and β-secretase cleavages. In cells with increased cholesterol content, the activation of the sterol-regulated proteolysis of APP requires exchange of cholesterol from the CE to the FC pool. Indeed, both biochemical and metabolic experiments in the cholesterol mutant cell lines indicate that increased levels of FC activate the generation of APP-C470 only when CE levels are reduced. This is particularly evident in 25RA cells under ACAT inhibition (Fig. 1), where APP-C470 could not be detected after 1 week of treatment, even when FC levels were as much as twofold higher than in untreated cells. Similar levels of FC were sufficient to generate APP-C470 in the absence of CEs (AC29 in Fig. 2; see mβ-CD alone). APP-C470 was visible in 25RA cells after 3 weeks of ACAT inhibition, which produced a net decrease in CE levels together with increased FC. This “metabolic requirement” suggests that there may be novel protein(s) that regulate APP processing in a “cholesterol-sensitive” manner. Lowering membrane cholesterol in neurons has been shown to enhance colocalization of APP and BACE1 in detergent-resistant membrane microdomains resulting in increased Aβ generation (Abad-Rodriguez et al. 2004). This is consistent with our findings that normalizing the unusually high FC levels in AC29 cells partially restores the capacity to generate Aβ in these cells (Fig. 2). Whether the sterol-dependent cleavage pathway of APP is active in neurons remains to be seen. It is possible that without proteasome inhibition, the endogenous intermediate product of this pathway, APP-C470, has remained unidentified until now.

Altered cholesterol distribution in cellular membranes might also affect intracellular membrane dynamics and APP processing independently of the novel, sterol-sensitive cleavage pathway. In this regard, it is interesting to note that statin treatment of cells, resulting in reduction in both CEs and FC, inhibits γ-secretase activity (Fassbender et al. 2001), while impaired NPC1 function, resulting in high endosomal FC–low CEs, also inhibits γ-secretase function (Burns et al. 2003; Runz et al. 2002). Moreover, it is possible that there may be more than one molecular mechanism connecting APP metabolism to ACAT activity and FC-to-CE ratio in cells. ACAT inhibitor treatment of cells with homeostatic cholesterol levels does not seem to promote accumulation of APP-C470 although C99, C83, and Aβ levels are all decreased. We have recently obtained evidence that ACAT inhibitors may affect APP trafficking in the early secretory pathway of normocholesterolemic cells (Huttunen and Kovacs, manuscript in preparation). How this is connected to the novel sterol-sensitive cleavage pathway of APP is currently unknown. Importantly though, ACAT activity may affect APP metabolism in the two key locations for cholesterol homeostasis, endosomal compartment and endoplasmic reticulum.

Recently, genetic screening has identified a polymorphism in *SOAT1*, the gene that encodes ACAT1, which is associated with low brain amyloid load and reduced risk for AD in the general population (Wollmer et al. 2003). In addition, analysis of lipid metabolism in the spinal cord of patients affected by amyotrophic lateral sclerosis (ALS) has revealed abnormal changes in sphingolipid metabolism together with abnormal accumulation of CE (Cutler et al. 2002). Therefore, in addition to atherosclerosis, CE metabolism appears to be linked to two different neurodegenerative disorders affecting central (AD) or peripheral (ALS) neurons. With regard to Alzheimer-like neurodegeneration, our results show that FC-to-CE ratios are directly connected to Aβ generation and cellular fate of APP holoprotein. Further mechanistic characterization of how subcellular cholesterol distribution modulates APP metabolism may eventually lead to the development of new therapeutic modalities for the treatment and/or prevention of AD, aimed at reducing Aβ generation.

NIH-PA Author Manuscript

NIH-PA Author Manuscript

NIH-PA Author Manuscript

Acknowledgements

We thank T.Y. Chang and C.C.Y. Chang (Dartmouth Medical School, Hanover, NH, USA) for the gift of cholesterol mutant cell lines, J.H. Harwood (Pfizer, Groton, CT, USA) for providing us with the ACAT inhibitor CP-113,818, and DJ. Selkoe and W.Xia (Center for Neurological Diseases, Brigham and Women's Hospital, Boston, MA, USA) for Aβ determinations. This work was supported by grants from the NIH-NINDS (D.M.K.), the Alzheimer's Association (L.P.), Helsingin Sanomat Centennial Foundation (H.J.H.) and Maud Kuistila Foundation (H.J.H.).

References

Abad-Rodriguez J, Ledesma MD, Craessaerts K, Perga S, Medina M, Delacourte A, et al. Neuronal membrane cholesterol loss enhances amyloid peptide generation. Journal of Cell Biology 2004;167:953–960. [PubMed: 15583033]

Abbenante G, Kovacs DM, Leung DL, Craik DJ, Tanzi RE, Fairlie DP. Inhibitors of beta-amyloid formation based on the beta-secretase cleavage site. Biochemical and Biophysical Research Communications 2000;268:133–135. [PubMed: 10652226]

Boerwinkle E, Visvikis S, Welsh D, Steinmetz J, Hanash SM, Sing CF. The use of measured genotype information in the analysis of quantitative phenotypes in man II. The role of the apolipoprotein E polymorphism in determining levels, variability, and covariability of cholesterol, beta-lipoprotein, and triglycerides in a sample of unrelated individuals. American Journal of Medical Genetics 1987;27:567–582. [PubMed: 3631131]

Brown MS, Goldstein JL. A proteolytic pathway that controls the cholesterol content of membranes, cells, and blood. Proceedings of the National Academy of Sciences of the United States of America 1999;96:11041–11048. [PubMed: 10500120]

Burns M, Gaynor K, Olm V, Mercken M, LaFrancois J, Wang L, et al. Presenilin redistribution associated with aberrant cholesterol transport enhances beta-amyloid production in vivo. Journal of Neuroscience 2003;23:5645–5649. [PubMed: 12843267]

Cadigan KM, Heider JG, Chang TY. Isolation and characterization of Chinese hamster ovary cell mutants deficient in acyl-coenzyme A:cholesterol acyltransferase activity. Journal of Biological Chemistry 1988;263:274–282. [PubMed: 3335499]

Chang TY, Chang CC, Ohgami N, Yamauchi Y. Cholesterol sensing, trafficking, and esterification. Annual Review of Cell and Developmental Biology 2006;22:129–157.

Corder EH, Saunders EH, Strittmatter WJ, Schmechel DE, Gaskell PG, Small GW, et al. Gene dose of apolipoprotein E type 4 allele and the risk of Alzheimer's disease in late onset families [see comments]. Science 1993;261:921–923. [PubMed: 8346443]

Cutler RG, Pedersen WA, Camandola S, Rothstein JD, Mattson MP. Evidence that accumulation of ceramides and cholesterol esters mediates oxidative stress-induced death of motor neurons in amyotrophic lateral sclerosis. Annals of Neurology 2002;52:448–457. [PubMed: 12325074]

Ehnholm C, Lukka M, Kuusi T, Nikkila E, Utermann G. Apolipoprotein E polymorphism in the Finnish population: gene frequencies and relation to lipoprotein concentrations. Journal of Lipid Research 1986;27:227–235. [PubMed: 3734624]

Fassbender K, Simons M, Bergmann C, Stroick M, Lutjohann D, Keller P, et al. Simvastatin strongly reduces levels of Alzheimer's disease beta-amyloid peptides Abeta 42 and Abeta 40 in vitro and in vivo. Proceedings of the National Academy of Sciences of the United States of America 2001;98:5856–5861. [PubMed: 11296263]

Fitzky BU, Moebius FF, Asaoka H, Waage-Baudet H, Xu L, Xu G, et al. 7-Dehydrocholesterol-dependent proteolysis of HMG-CoA reductase suppresses sterol biosynthesis in a mouse model of Smith-Lemli-Opitz/RSH syndrome. Journal of Clinical Investigation 2001;108:905–915. [PubMed: 11560960]

Frears ER, Stephens DJ, Walters CE, Davies H, Austen BM. The role of cholesterol in the biosynthesis of beta-amyloid. Neuroreport 1999;10:1699–1705. [PubMed: 10501560]

Glenner GG, Wong CW. Alzheimer's disease: Initial report of the purification and characterization of a novel cerebrovascular amyloid protein. Biochemical and Biophysical Research Communications 1984;120:885–890. [PubMed: 6375662]

NIH-PA Author Manuscript

NIH-PA Author Manuscript

NIH-PA Author Manuscript

Grimm MO, Grimm HS, Patzold AJ, Zinser EG, Halonen R, Duering M, et al. Regulation of cholesterol and sphingomyelin metabolism by amyloid-beta and presenilin. Nature Cell Biology 2005;7:1118–1123.

Haass C. Take five-BACE and the gamma-secretase quartet conduct Alzheimer's amyloid beta-peptide generation. EMBO Journal 2004;23:483–488. [PubMed: 14749724]

Hutter-Paier B, Huttunen HJ, Puglielli L, Eckman CB, Kim DY, Hofmeister A, et al. The ACAT inhibitor CP-113,818 markedly reduces amyloid pathology in a mouse model of Alzheimer's disease. Neuron 2004;44:221–238.

Huttunen HL, Greco C, Kovacs DM. Knockdown of ACAT-1 reduces amyloidogenic processing of APP. FEBS letters 2007a;581:1688–1692. [PubMed: 17412327]

Huttunen HJ, Guenette SY, Peach C, Greco C, Xia W, Kim DY, et al. HtrA2 regulates beta-amyloid precursor protein (APP) metabolism through endoplasmic reticulum-associated degradation. Journal of Biological Chemistry 2007b;282:28285–28295. [PubMed: 17684015]

Jarvik GP, Wijsman EM, Kukull W, Schellenberg GD, Yu C, Larson EB. Interactions of apolipoprotein E genotype, total cholesterol level, age, and sex in prediction of Alzheimer's disease: a case-control study. Neurology 1995;45:1092–1096. [PubMed: 7783869]Medline.

Jick H, Zornberg GL, Jick SS, Seshadri S, Drachman DA. Statins and the risk of dementia. Lancet 2000;356:1627–1631. [PubMed: 11089820]

Kang J, Lemaire HG, Unterbeck A, Salbaum JM, Masters CL, Grzeschik KE, et al. The precursor of Alzheimer's disease amyloid A4 protein resembles a cell-surface receptor. Nature 1987;325:733–736. [PubMed: 2881207]

Koudinov AR, Berezov TT, Kumar A, Koudinova NV. Alzheimer's amyloid beta interaction with normal human plasma high density lipoprotein: Association with apolipoprotein and lipids. Clinica Chimica Acta 1998;270:75–84.

Kuo YM, Emmerling MR, Bisgaier CL, Essenburg AD, Lampert HC, Drumm D, et al. Elevated low-density lipoprotein in Alzheimer's disease correlates with brain A beta 1–42 levels. Biochemical and Biophysical Research Communications 1998;252:711–715. [PubMed: 9837771]

Lee SJ, Liyanage U, Bickel PE, Xia W, Lansbury PT Jr, Kosik KS. A detergent-insoluble membrane compartment contains A beta in vivo. Nature Medicine 1998;4:730–734.

Liu Q, Zerbinatti CV, Zhang J, Hoe HS, Wang B, Cole SL, et al. Amyloid precursor protein regulates brain apolipoprotein E and cholesterol metabolism through lipoprotein receptor LRP1. Neuron 2007;56:66–78. [PubMed: 17920016]

Murata M, Peranen J, Schreiner R, Wieland F, Kurzchalia TV, Simons K. VIP21/caveolin is a cholesterol-binding protein. Proceedings of the National Academy of Sciences of the United States of America 1995;92:10339–10343. [PubMed: 7479780]

Notkola IL, Sulkava R, Pekkanen J, Erkinjuntti T, Ehnholm C, Kivinen P, et al. Serum total cholesterol, apolipoprotein E epsilon 4 allele, and Alzheimer's disease. Neuroepidemiology 1998;17:14–20. [PubMed: 9549720]

Parkin ET, Hussain I, Karran EH, Turner AJ, Hooper NM. Characterization of detergent-insoluble complexes containing the familial Alzheimer's disease-associated presenilins. Journal of Neurochemistry 1999;72:1534–1543. [PubMed: 10098859]

Podlisny MB, Tolan DR, Selkoe DJ. Homology of the amyloid beta protein precursor in monkey and human supports a primate model for beta amyloidosis in Alzheimer's disease. American Journal of Pathology 1991;138:1423–1435. [PubMed: 1905108]

Porter JA, Young KE, Beachy PA. Cholesterol modification of hedgehog signaling proteins in animal development [see comments] [published erratum appears in Science 1996 Dec 6;274(5293):1597]. Science 1996;274:255–259. [PubMed: 8824192]

Puglielli L, Konopka G, Pack-Chung E, Ingano LA, Berezovska O, Hyman BT, et al. Acyl-coenzyme A: Cholesterol acyltransferase modulates the generation of the amyloid beta-peptide. Nature Cell Biology 2001;3:905–912.

Puglielli L, Tanzi RE, Kovacs DM. Alzheimer's disease: The cholesterol connection. Nature Neuroscience 2003;6:345–351.

NIH-PA Author Manuscript

NIH-PA Author Manuscript

NIH-PA Author Manuscript

Refolo LM, Wittenberg IS, Friedrich VL Jr, Robakis NK. The Alzheimer amyloid precursor is associated with the detergent-insoluble cytoskeleton. Journal of Neuroscience 1991;11:3888–3897. [PubMed: 1683901]

Refolo LM, Pappolla MA, Malester B, LaFrancois J, Bryant-Thomas T, Wang R, et al. Hypercholesterolemia accelerates the Alzheimer's amyloid pathology in a transgenic mouse model. Neurobiology of Disease 2000;7:321–331. [PubMed: 10964604]

Refolo LM, Pappolla MA, LaFrancois J, Malester B, Schmidt SD, Thomas-Bryant T, et al. A cholesterol-lowering drug reduces beta-amyloid pathology in a transgenic mouse model of Alzheimer's disease. Neurobiology of Disease 2001;8:890–899. [PubMed: 11592856]

Runz H, Rietdorf J, Tomic I, de Bernard M, Beyreuther K, Pepperkok R, et al. Inhibition of intracellular cholesterol transport alters presenilin localization and amyloid precursor protein processing in neuronal cells. Journal of Neuroscience 2002;22:1679–1689. [PubMed: 11880497]

Schmechel DE, Saunders AM, Strittmatter WJ, Crain BJ, Hulette CM, Joo SH, et al. Increased amyloid β-peptide deposition in cerebral cortex as a consequence of apolipoprotein E genotype in late-onset Alzheimer disease. Proceedings of the National Academy of Sciences of the United States of America 1993;90:9649–9653. [PubMed: 8415756]

Sever N, Yang T, Brown MS, Goldstein JL, DeBose-Boyd RA. Accelerated degradation of HMG CoA reductase mediated by binding of insig-1 to its sterol-sensing domain. Molecular Cell 2003;11:25–33. [PubMed: 12535518]

Simons M, Keller P, De Strooper B, Beyreuther K, Dotti CG, Simons K. Cholesterol depletion inhibits the generation of beta-amyloid in hippocampal neurons. Proceedings of the National Academy of Sciences of the United States of America 1998;95:6460–6464. [PubMed: 9600988]

Tanzi RE, Gusella JF, Watkins PC, Bruns GA, George-Hyslop P St, Van Keuren ML, et al. Amyloid beta protein gene: cDNA, mRNA distribution, and genetic linkage near the Alzheimer locus. Science 1987;235:880–884. [PubMed: 2949367]

Thiele C, Hannah MJ, Fahrenholz F, Huttner WB. Cholesterol binds to synaptophysin and is required for biogenesis of synaptic vesicles. Nature Cell Biology 2000;2:42–49.

Wollmer MA, Staffer JR, Tsolaki M, Grimaldi LM, Lutjohann D, Thal D, et al. Genetic association of acyl-coenzyme A: Cholesterol acyltransferase with cerebrospinal fluid cholesterol levels, brain amyloid load, and risk for Alzheimer's disease. Molecular Psychiatry 2003;8:635–638. [PubMed: 12851640]

Wolozin B, Kellman W, Ruosseau P, Celesia GG, Siegel G. Decreased prevalence of Alzheimer disease associated with 3-hydroxy-3-methyglutaryl coenzyme A reductase inhibitors. Archives of Neurology 2000;57:1439–1443. [PubMed: 11030795]

Yang T, Espenshade PJ, Wright ME, Yabe D, Gong Y, Aebersold R, et al. Crucial step in cholesterol homeostasis: Sterols promote binding of SCAP to INSIG-1, a membrane protein that facilitates retention of SREBPs in ER. Cell 2002;110:489–500. [PubMed: 12202038]

NIH-PA Author Manuscript
NIH-PA Author Manuscript
NIH-PA Author Manuscript

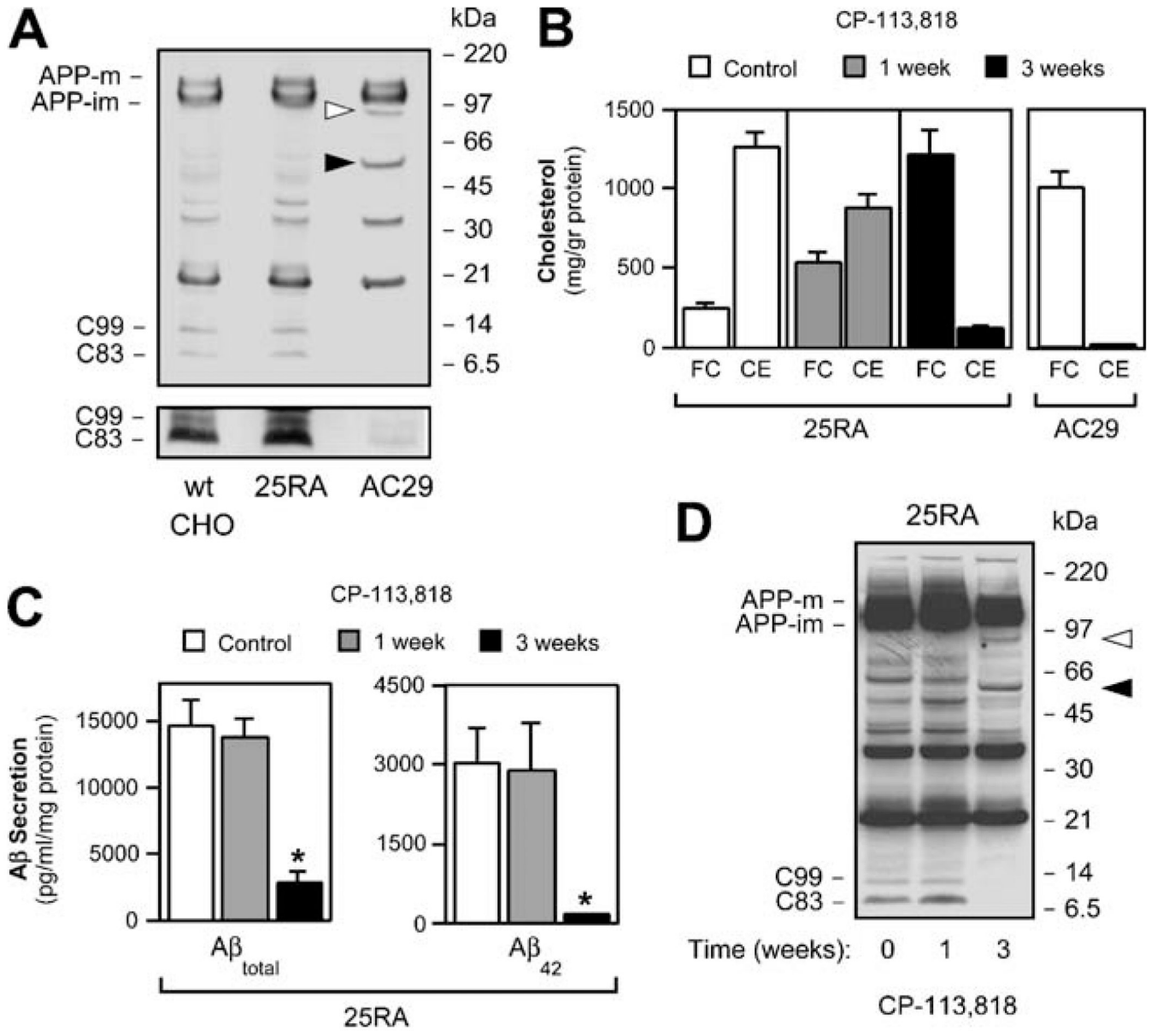

Fig. 1.

ACAT inhibition alters normal proteolytic processing of APP. **a** Western blot analysis of wild-type CHO, 25RA, and AC29 cell lines stably transfected with APP. *Arrowheads* indicate two novel APP-CTFs of ~85- and ~55-kDa, which are only visible in AC29 cells. The overexposed *inset* illustrates a marked reduction in C99 and C83 levels in AC29 cells. Antibody: C7, against the C-terminus of APP. **b** 25RA cells require 3 weeks of treatment with the ACAT inhibitor CP-113,818 (5 μM) to reach an FC-to-CE ratio similar to that found in AC29 cells. **c** The shift of cholesterol from the pool of CE to that of FC in 25RA cells almost completely abolished the secretion of both $A\beta_{total}$ and $A\beta_{42}$, as shown in a sandwich ELISA assay, and d was accompanied by the appearance of both ~55- and ~85-kDa APP-CTFs (*arrowheads*). A marked reduction in the steady-state levels of both C99 and C83 is also evident. Antibody: C7, against the C-terminus of APP. Values are the mean±SD of at least three independent experiments, *asterisks*, $p<0.05$

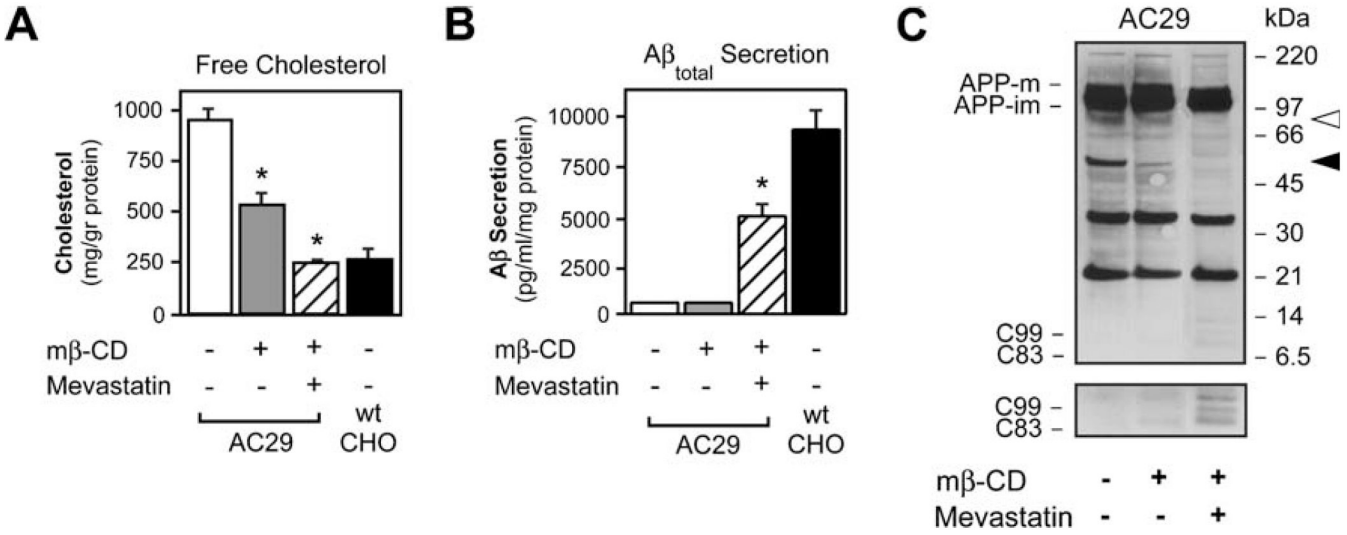

Fig. 2.

Both elevated FC and decreased CE are required for altered proteolytic processing of APP in AC29 cells. AC29 cells stably transfected with APP were treated ad equilibrium with methyl β-cyclodextrin (*mβ-CD*; 1 mM) and/or mevastatin (5 μM) to reduce FC levels. **a** Only the combination of mβ-CD and mevastatin reduced FC levels to those found in wild-type CHO cells. mβ-CD alone was able to partially reduce but did not normalize FC levels. **b** Normalization of FC increased but did not normalize the secretion of Aβ into the media, reaching ~50% of total Aβ secreted by wild-type CHO cells. **c** Western blot showing that both the ~55- and ~85-kDa APP-CTFs (shown by *arrowheads*) disappeared after normalization of FC levels (mβ-CD + mevastatin). This was accompanied by an increase in the steady-state levels of both C99 and C83. Antibody: C7, against the C-terminus of APP. Values are the mean ±SD of at least three separate experiments. *asterisks*, $p<0.05$

NIH-PA Author Manuscript
NIH-PA Author Manuscript
NIH-PA Author Manuscript

NIH-PA Author Manuscript
NIH-PA Author Manuscript
NIH-PA Author Manuscript

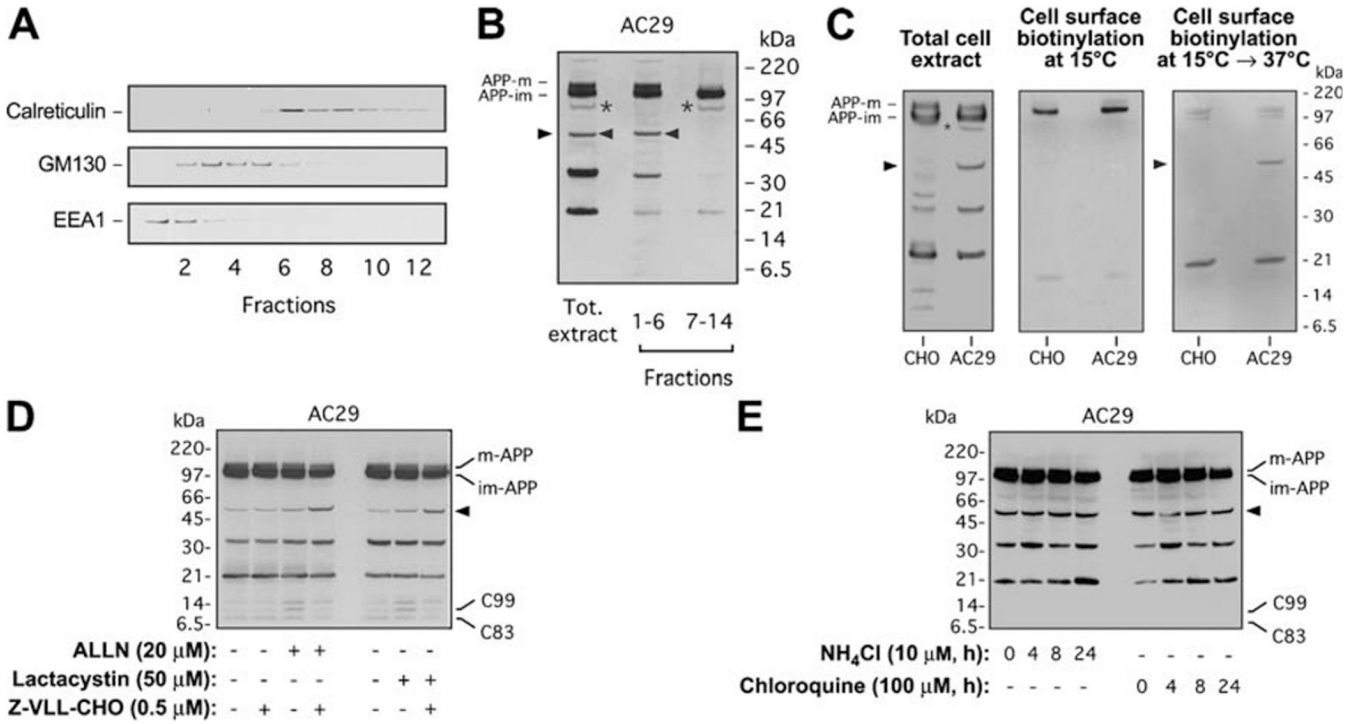

Fig. 3.

Sterol-sensitive cleavage of APP occurs in an endosomal compartment and is followed by proteasomal degradation in AC29 cells. **a** Cell membranes from AC29 cells stably transfected with APP were subjected to subcellular fractionation in a continuous 8–34% OptiPrep gradient. Migration of ER (calreticulin), Golgi (GM130), and early endosome (EEA1) markers in a typical gradient is shown. **b** Western blot analysis of APP processing was done in pooled fractions to increase the yield. 85-kDa (*asterisks*) and 55-kDa (*arrowheads*) APP-CTFs are indicated; mature (*APP-m*) and immature (*APP-im*) APP are also shown. APP-m was only detected in the fractions containing the Golgi or endosomal markers. Antibody: C7, against the C-terminus of APP. **c** Wild-type CHO and AC29 cells stably transfected with APP (APP expression shown in total cell extract blot on the left) were subjected to cell surface biotinylation and Western blot analysis to detect cell surface APP. Biotinylation at 15°C did not reveal generation of the 55-kDa APP-CTF at the cell surface (blot in the middle). To test if the 55-kDa APP-CTF is generated after internalization of APP holoprotein on the cell surface, cells were replaced at 37°C following biotinylation at 15°C (blot on the right). Antibody: C7, against the C-terminus of APP. **d** AC29 cells stably transfected with APP were treated with proteasome inhibitors ALLN (20 μM) or lactacystin (50 μM) and the β-secretase inhibitor Z-VLL-CHO (0.5 μM) for 24 h prior to Western blot analysis. Proteasome inhibition stabilized the 55-kDa APP-CTF and was able to activate the β-cleavage of the 55-kDa APP-CTF. **e** AC29 cells stably transfected with APP were treated with lysosomal inhibitors ammonium chloride (NH_4Cl, 10 μM) or chloroquine (100 μM) for indicated times prior to Western blot analysis. Lysosomal inhibitors had no effect on the steady-state levels of the 55-kDa APP-CTF. Antibody: C7, against the C-terminus of APP

NIH-PA Author Manuscript

NIH-PA Author Manuscript

NIH-PA Author Manuscript

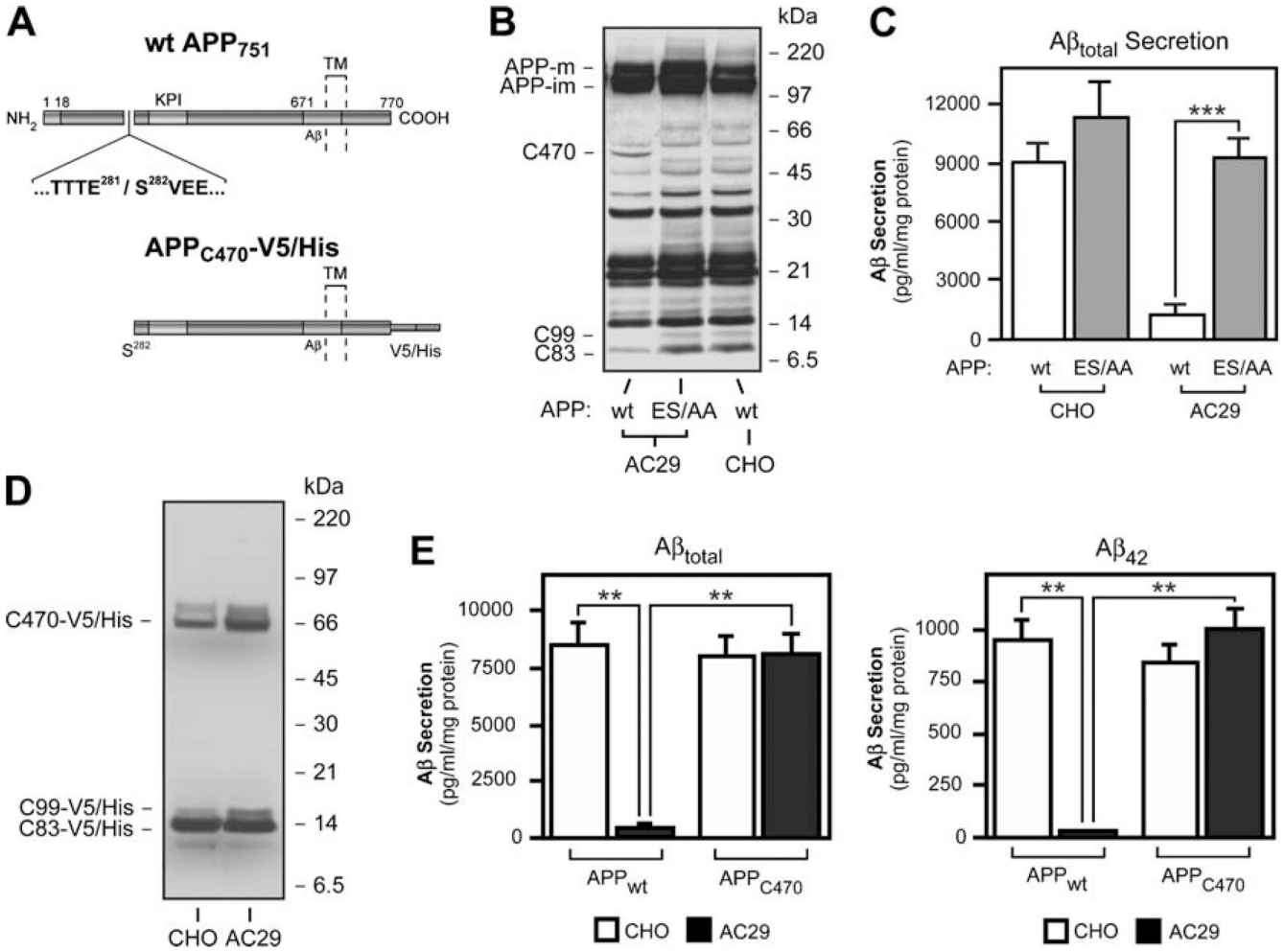

Fig. 4.

The 55-kDa APP-CTF is generated by cleavage of APP holoprotein at Glu281 and precludes α- and β-cleavages and Aβ generation in AC29 cells. **a** Schematic view of APP_{751} illustrating the site of Glu281 cleavage. The location of Aβ region and the Kunitz-type proteinase inhibitor (*KPI*) domain are indicated. The *dotted lines* indicate the single transmembrane (*TM*) region of APP. Below is a schematic view of APP_{C470}-V5/His, an APP deletion mutant lacking the N-terminal 281 amino acids fused with a V5/His tag at the C-terminus. **b** Glu281 and Ser282 were mutagenized to alanine residues to abolish the generation of C470. Western blot analysis of AC29 cells stably transfected with the new construct, APP (ES/AA), shows that mutagenesis of the Glu281 cleavage site reactivated C99 and C83 production. Antibody: C7, against the C-terminus of APP. **c** AC29 cells stably transfected with APP (ES/AA) fully recovered their ability to generate and secrete Aβ into the media. Aβ levels in the media were detected by sandwich ELISA. **d** Western blot analysis showing that APP_{C470}-V5/His is processed normally in AC29 cells, in terms of C83 and C99 production by α and β cleavages. Antibody: C7, against the C-terminus of APP. **e** AC29 cells stably expressing APP_{C470}-V5/His recovered their ability to generate Aβ to normal levels, as shown by a sandwich ELISA. Values represent the mean ±SD of at least three independent experiments. *,$p<0.05$; **, $p<0.01$; ***, $p<0.001$